

# Hybrid Water Electrolysis: A New Sustainable Avenue for Energy-Saving Hydrogen Production

Zhijie Chen<sup>1</sup>, Wei Wei<sup>1</sup>, Lan Song<sup>2</sup>, Bing-Jie Ni<sup>1,\*</sup>

<sup>1</sup> Centre for Technology in Water and Wastewater, School of Civil and Environmental Engineering, University of Technology Sydney, NSW, 2007, Australia

<sup>2</sup> School of Environmental Science and Engineering, Southern University of Science and Technology, Shenzhen, 518055, PR China



## ARTICLE INFO

### Keywords:

Hybrid water electrolysis  
Hydrogen evolution reaction  
Organic oxidation reaction  
Electrocatalysts  
Sustainable energy

## ABSTRACT

Developing renewable energy-driven water splitting for sustainable hydrogen production plays a crucial role in achieving carbon neutrality. Nevertheless, the efficiency of traditional pure water electrolysis is severely hampered by the anodic oxygen evolution reaction (OER) due to its sluggish kinetics. In this context, replacing OER with thermodynamically more favorable oxidation reactions via hybrid water electrolysis becomes an energy-saving hydrogen production scheme. Here, the recent advances in hybrid water electrolysis are critically reviewed. First, the fundamentals of electrochemical oxidation of typical organic molecules such as urea, hydrazine, and biomass are presented. Then, the recent achievements in electrocatalysts for hybrid water electrolysis are introduced, emphasizing the outline of catalyst design strategies and the correlation between catalyst structure and performance. Finally, future perspectives for a sustainable hydrogen economy are proposed.

## 1. Introduction

The ever-growing global energy demand links with the depletion of fossil fuels (e.g., coal, gasoline, natural gas) and the detrimental environmental impact (You and Sun, 2018; Zhao et al., 2020b). In such circumstances, developing sustainable and renewable energy to realize a low carbon energy system is an inevitable trend (Chen et al., 2021b; Liao et al., 2019). Hydrogen, with carbon-free features and high gravimetric energy density, has been perceived as an alternate fuel to support the green and sustainable energy system (Ali and Shen, 2020; Chen et al., 2021d; Xu et al., 2020; Xue et al., 2022; Zhao et al., 2020c). Currently, producing hydrogen from renewable energy (e.g., solar energy, wind)-driven water electrolysis is gaining popularity in the world due to its environmental friendliness, high hydrogen production efficiency, and sustainability (Anantharaj and Aravindan, 2020; Chen et al., 2019).

Pure water electrolysis (PWE) consists of two half-reactions, namely, the anodic oxygen evolution reaction (OER) and the cathodic hydrogen evolution reaction (HER). Unlike the HER that follows a simple two-electron process, the theoretical four-electron OER with inherent sluggish kinetics remains a central barrier to advance PWE systems (Song et al., 2020). Although significant efforts have been achieved in developing efficient electrocatalysts (Chen et al., 2021c; Wang et al., 2019b; Yang et al., 2021a; Zhang et al., 2019), OER overpotentials of advanced catalysts for achieving a current density of  $10 \text{ mA cm}^{-2}$  are still about 0.2 - 0.4 V; thus, the unfavorable OER increases the electricity input of

water electrolyzers. In addition, the simultaneous production of oxygen and hydrogen gases would induce gas crossover, although membranes are employed in electrolyzers during the long-term operation, raising a safety concern (Martínez et al., 2020). At the same time, oxygen gas produced at the anode shows meager market value, which is usually vented instead of captured for any valuable purposes (Luo et al., 2021). The previous study also suggests that reactive oxygen species generated at the anode during the electrolysis process will damage the membrane and thus increase the running cost of electrolyzers (Berger et al., 2014). Therefore, the high running cost of PWE is a significant drawback that limits the production of hydrogen on an industrial scale.

It is sensible to integrate HER with thermodynamically more favorable and value-added electrooxidation reactions to address these issues. The hybrid water electrolyzers would decrease the cost by reducing energy consumption, and some reactions can even realize adding market value via producing economically viable products at the anode (You et al., 2018). Recently, hybrid water electrolysis systems have attracted growing research interest. Many electrooxidation reactions are well explored as the anode reaction (Zhang et al., 2021a; Zhang et al., 2021b; Zhao et al., 2021a; Zhao et al., 2021b). For example, Wang et al. found that coupling urea oxidation reaction (UOR) with HER could realize energy-saving hydrogen production because the UOR/HER hybrid system took a lower potential for achieving the current density of  $100 \text{ mA cm}^{-2}$  than PWE (1.68 vs. 1.91 V) (Wang et al., 2020). It should be noticed that the coupling between cathodic and anodic reactions would

\* Corresponding author.

E-mail address: [bingjeni@gmail.com](mailto:bingjeni@gmail.com) (B.-J. Ni).

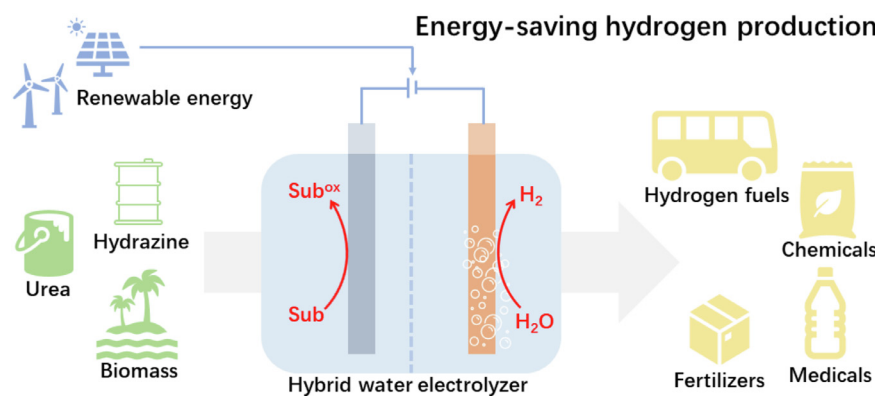


**Figure 1.** Schematic illustration of energy-saving hydrogen production via hybrid water electrolysis, which is composed of electrooxidation of the substrate molecule (sub) into sub<sup>ox</sup> with hydrogen generation at the cathode.

present conflicts since the two chosen electrochemical half-reactions may require various reaction conditions (e.g., pH values, solvents, reaction rates) (Wang et al., 2021a). Therefore, it is necessary to select suitable oxidation reactions based on the electrochemical principles of the paired electrocatalytic reactions. Of equal importance, designing cost-effective electrocatalysts is required to realize an efficient electrocatalytic process.

This review aims to provide an overview of hybrid water electrolysis, which performs water splitting paired with alternative oxidation reactions for energy-saving hydrogen production. First, the fundamentals of typical electrochemical oxidation reactions (e.g., biomass oxidation, UOR, hydrazine oxidation) are discussed. After that, recent achievements in electrocatalysts for alternative electrooxidation reactions are introduced, emphasizing the design of catalysts and the catalyst property-performance correlation. At last, perspectives in this field for a sustainable hydrogen economy are pointed out.

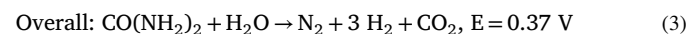
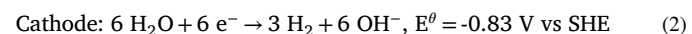
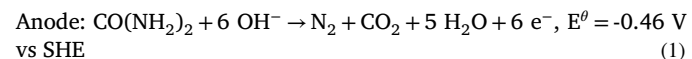
## 2. Fundamentals of alternative oxidation reaction coupled water electrolysis

Theoretically, PWE for hydrogen production requires an applied voltage of 1.23 V. However, due to the real electrolyzer's reaction hindrances, a higher voltage (~ 2.0 V) is needed for driving PWE (Martínez et al., 2020). Thus, an alternative to OER should be thermodynamically more favorable than OER, which usually refers to the electrochemical oxidation of organic substrates. Several requirements should be met to construct an energy-saving hybrid water electrolysis system: (1) the selected organic substrates should have a high solubility in water at room temperature; and (2) the oxidation of organic substrates possess a lower onset potential compared to OER (You et al., 2016). The electrochemical oxidation of small molecules like urea and hydrazine fulfills these criteria (Du et al., 2020; Li et al., 2020). Apart from the two prerequisites, the transformation of the organic molecules during the electrooxidation process also can lead to value-added products which are expensive or difficult to be obtained by conventional chemical processing (Huang et al., 2019). In this context, the electrooxidation of biomass or biomass derivatives (e.g., short-chain alcohols) is a favorable choice to simultaneously obtain platform chemicals and sustainable hydrogen gas (Li et al., 2021b). Such biomass-coupled water electrolysis systems will significantly cut the dependence on traditional fossil fuels, usually employed to produce industrially important chemicals. The most widely explored electrochemical oxidation reactions are analyzed (Figure 1), especially the reaction mechanisms.

### 2.1. Electrochemical oxidation of urea

Urea is widely present in industrial wastewater and human/animal urine (Hu et al., 2020). Thus, hybridizing UOR with water electrolysis could realize ecological protection and clean energy generation by

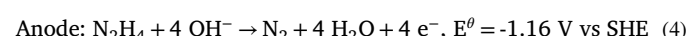
effectively producing H<sub>2</sub> and purifying urea-rich wastewater or urine (Gnana Kumar et al., 2020). The reaction principles of the UOR/HER hybrid system follow equations (1-3) in the alkaline electrolyte (SHE: standard hydrogen electrode) (Sun and Ding, 2020):



Therefore, the urea-assisted water electrolysis takes a much lower theoretical overall voltage to produce H<sub>2</sub> than PWE. For example, the NP-Ni<sub>0.70</sub>Fe<sub>0.30</sub>||NP-Ni<sub>0.70</sub>Fe<sub>0.30</sub> couple could realize 10 mA cm<sup>-2</sup> at 1.55 V in the 1 M KOH with 0.33 M urea, which was significantly lower than that in PWE (1.68 V) (Cao et al., 2020). Ni-based catalysts are currently the best for UOR, even compared with noble metals like Pt and Rh (Luo et al., 2021). The investigation of the UOR mechanism and kinetics on Ni-based electrocatalysts in an alkaline medium shows that urea oxidation occurs after the generation of NiOOH under the electrooxidation conditions, which reacts with urea molecules and regenerates active sites for further adsorption/desorption of intermediates. A recent study reveals a lattice-oxygen-involved UOR mechanism on Ni<sup>4+</sup> active sites, and this process shows significantly faster reaction kinetics than the conventional NiOOH mechanism (Figure 2a) (Zhang et al., 2019). It is noteworthy that the UOR follows the diffusion and kinetically controlled mechanisms, evidenced by experimental results (Han et al., 2020). Hence, it is necessary to design suitable experimental conditions to achieve a high reaction efficiency, including urea concentration, pH value, etc. As mentioned above, UOR is a six-electron process with multiple gas evolution steps, resulting in intrinsically sluggish kinetics and high overpotentials (Qian et al., 2020). Therefore, high-performance Ni-based electrocatalysts are required to lower the reaction energy barriers. In general, the design of UOR catalysts mainly focuses on engineering active sites, increasing Ni valence state, and designing efficient mass/charge transport structure, which will be discussed hereinafter.

### 2.2. Electrochemical oxidation of hydrazine

Hydrazine, a typical carbon-free fuel and aqueous pollutant can also be electrochemically oxidized at a lower potential than OER. Furthermore, the hydrazine oxidation reaction (HzOR) only produces nitrogen without carbon-based emissions (Liu et al., 2020c). These advantages indicate that HzOR has a great potential to replace OER for water electrolysis. The reaction principles of the HzOR/HER system in alkaline solution follow equations (4-6) (Liu et al., 2020a; Wang et al., 2019c):



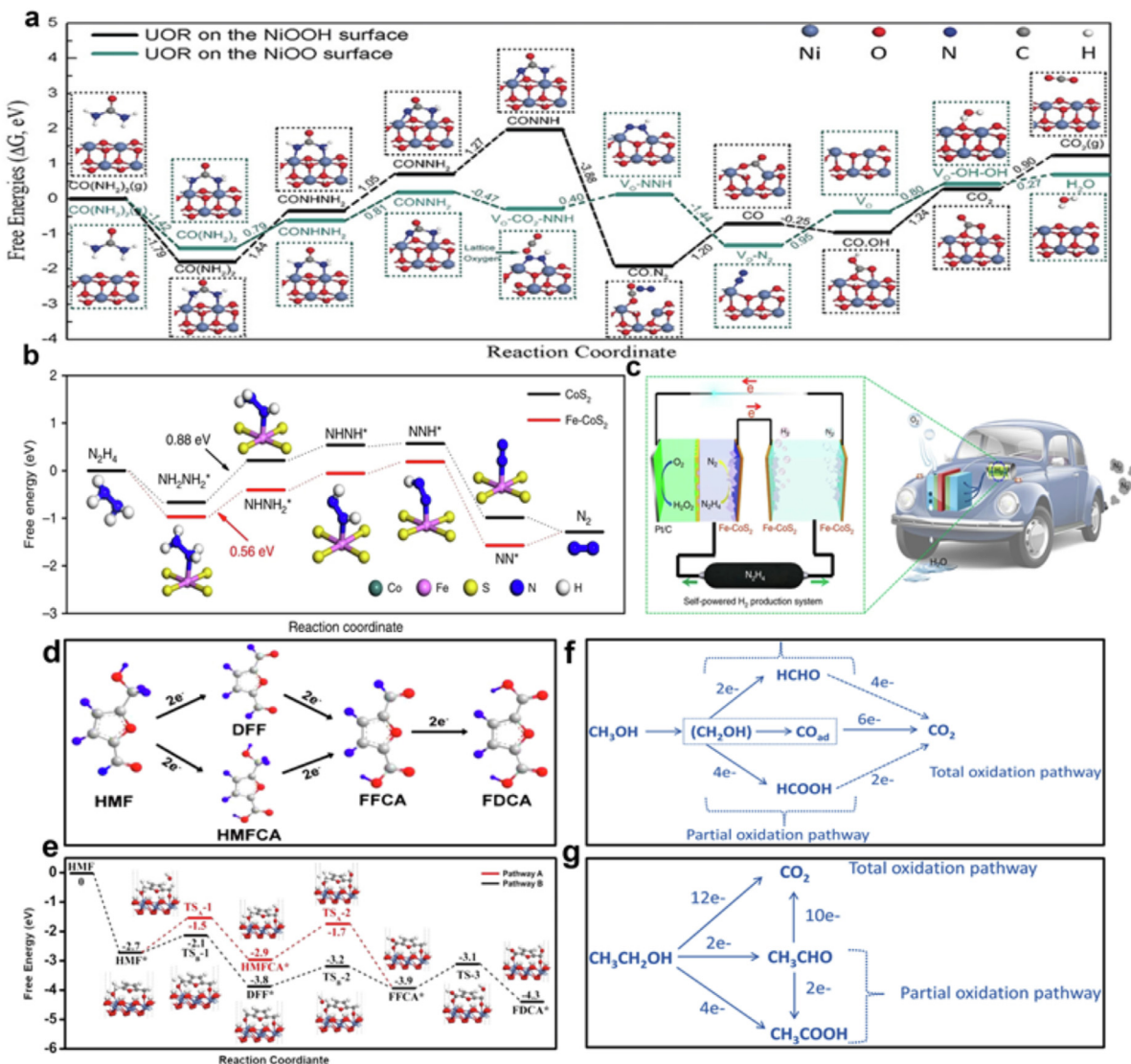
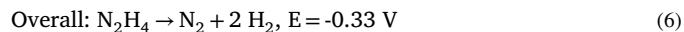
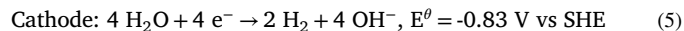


**Figure 2.** (a) The Gibbs free energy profiles and the reaction pathways of UOR on the NiOOH and NiOO surfaces (Zhang et al., 2019). Reprinted with permission from Copyright 2019, Wiley-VCH. (b) Free energy profiles of HzOR on the CoS<sub>2</sub> and Fe-CoS<sub>2</sub> surfaces. Insets show the most stable adsorption configurations of intermediates on the Fe-CoS<sub>2</sub> surface. (c) Scheme of a self-powered hydrogen generation system integrating a HzOR and a DHZFC unit (Liu et al., 2018). Reprinted with permission from Copyright 2018, Nature Publishing Group. (d) Scheme of two possible pathways for the HMF electrooxidation (C gray, H blue, O red) (Xie et al., 2021). Reprinted with permission from Copyright 2021, Wiley-VCH. (e) Energy profiles of HMF oxidation to FDCA on the NiOOH surface, Pathway A means the HMFCA-pathway, and Pathway B is the DFF-pathway (C gray, H white, O red, Ni blue) (Lu et al., 2021). Reprinted with permission from Copyright 2021, Wiley-VCH. (f) Mechanistic illustration of the electrooxidation of methanol; and (g) Mechanistic illustration of the electrooxidation of ethanol (Ozoemena, 2016). Reprinted with permission from Copyright 2016, Royal Society of Chemistry. All reprinted permissions are listed in the Supplementary Information.



Compared with PWE, the hydrazine-assisted water splitting only takes a much lower theoretical overall voltage for H<sub>2</sub> production. Recently, Du et al. found that the presence of 0.02 M hydrazine in the 1.0 M KOH solution could decrease the required voltage to attain 15 mA cm<sup>-2</sup> (0.63 vs. 1.97 V), using the bifunctional Ni@Pd–Ni alloy NAs as the anode and the cathode (Du et al., 2019). Notwithstanding, external energy is required in the current HzOR/HER system, which is a considerable obstacle for practical applications. As a result, the key to realizing efficient HzOR remains the rational design of cost-effective electrocatalysts for the activation of N<sub>2</sub>H<sub>4</sub> and its dehydrogenation to N<sub>2</sub>. Based on density functional theory (DFT) calculations, HzOR involves six elementary steps. The adsorption of N<sub>2</sub>H<sub>4</sub> and des-

orption of N<sub>2</sub> are the first and the final steps, separately. Each of the other four steps consists of forming one electron and one proton (**Figure 2b**). The potential determining steps (PDS) for both CoS<sub>2</sub> and Fe-CoS<sub>2</sub> are the dehydrogenation of \*NH<sub>2</sub>NH<sub>2</sub> (Liu et al., 2018). Differently, a more recent study suggests that the dehydrogenation of \*NHNH to \*N<sub>2</sub>H is the PDS for the Co<sub>3</sub>N catalyst, while the desorption process of \*N<sub>2</sub> to N<sub>2</sub> is the PDS for the P, W co-doped Co<sub>3</sub>N counterpart (Liu et al., 2020c). Therefore, the HzOR mechanism highly depends on the catalysts, and more experimental and computational studies are needed to uncover the reaction mechanisms for the design of efficient catalysts.

Beyond external electricity-driven HzOR assisted water electrolysis, it is more attractive to integrate direct hydrazine fuel cells (DHzFCs) with the HzOR assisted water electrolyzers. As the primary consumable in the self-powered H<sub>2</sub> production system, hydrazine is the fuel of DHzFC and the splitting target (**Figure 2c**) (Liu et al., 2018). With-

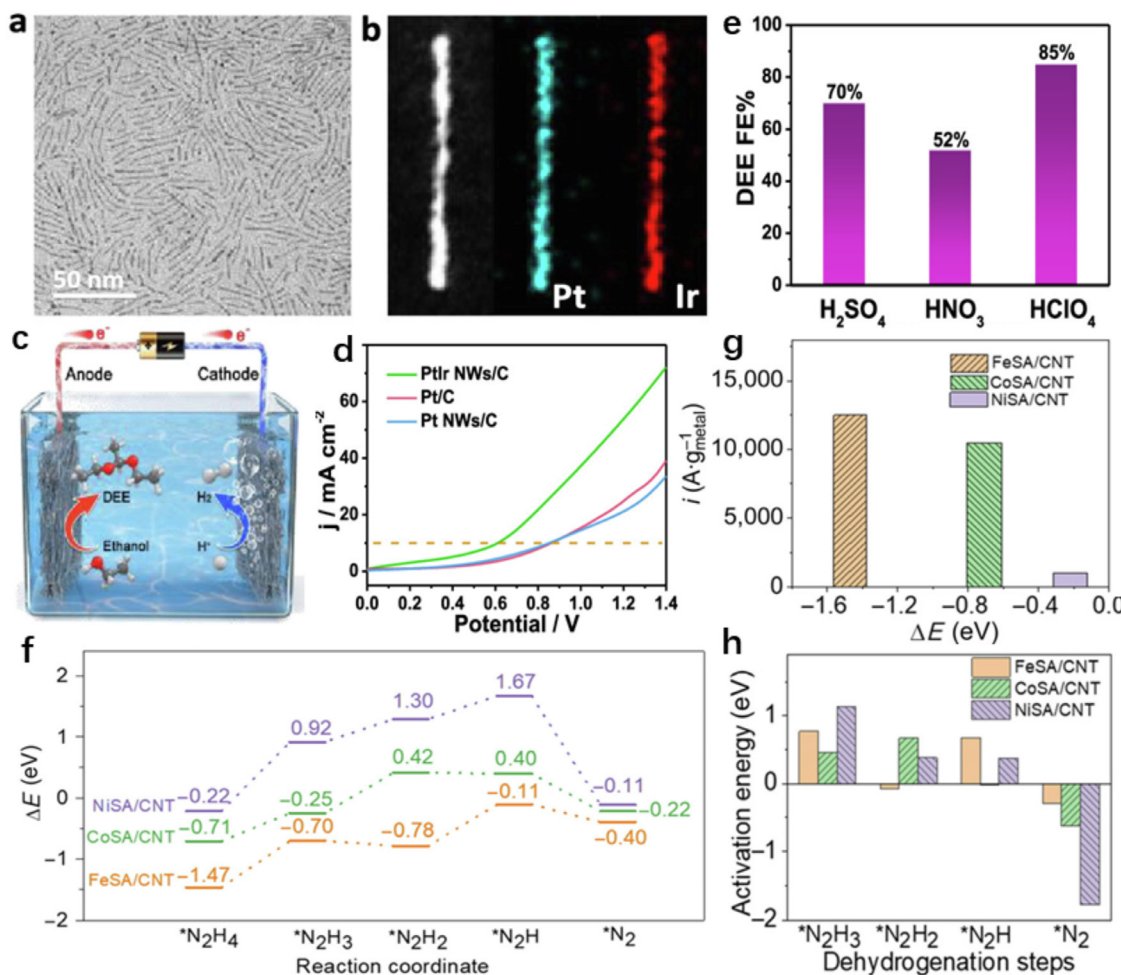


**Figure 3.** (a) Transmission electron microscopy (TEM) image, and (b) scanning TEM (STEM) image and the corresponding energy-dispersive spectroscopy (EDS) elemental mappings of PtIr NWs. (c) Schematic of the electrooxidation of ethanol to DEE and hydrogen generation electrolyzer. (d) LSV of the PtIr NWs/C // PtIr, Pt/C // Pt/C, and Pt NWs/C // Pt NWs/C cells in 0.5 M  $\text{H}_2\text{SO}_4$  ethanol electrolyte. (e) FEs of DEE in different acids at an applied voltage of 1.4 V (Yin et al., 2021). Reprinted with permission from Copyright 2021, American Chemical Society. (f) The reaction path of HzOR on different MSA/CNT catalysts. (g) Comparison of the  $\Delta E(^{*}\text{N}_2\text{H}_4)$  and current density at 0.524 V under  $\text{N}_2$  purged 1.0 M KOH + 0.1 M  $\text{N}_2\text{H}_4$  electrolyte. (h) The energy barrier of each dehydrogenation step on the MSA/CNT catalysts. (Zhang et al., 2021a). Reprinted with permission from Copyright 2021, Springer Nature.

out external powers, the hybrid system can realize efficient hydrogen production (9.95 mmol  $\text{h}^{-1}$ ).

### 2.3. Electrochemical oxidation of biomass (derivatives)

Biomass or biomass derivatives-assisted water splitting involves a complex oxidation process. The organic substrates can be totally oxidized into  $\text{CO}_2$  ( $\text{CO}_3^{2-}$ ) or partially oxidized into value-added chemicals (Bender et al., 2020). The oxidative products are tightly linked with the applied electrocatalysts and electrolytes. For example, the oxidation of glycerol can produce 1,3-dihydroxyacetone, tartaric acid, mesoxalic acid, glyoxylic acid, and  $\text{CO}_2$  with Au as the catalyst. In contrast, tartaric acid, glycolic acid, glyoxylic acid, formic acid, and  $\text{CO}_2$  can be obtained with Pt catalyst in 0.1 M NaOH (Gomes and Tremiliosi-Filho, 2011). Hence, biomass (derivatives) oxidation mechanisms are pretty complicated in reaction selectivity, which should be carefully explored on a case-by-case basis. In this part, the electrooxidation of several typical biomass (derivatives) is analyzed, including 5-hydroxymethylfurfural (HMF) and small-molecule alcohols (i.e., methanol, ethanol). Recent advances in the electrooxidation of other biomass (derivatives) (e.g., glucose, glycerol) could be found in several reviews (Fan et al., 2020; Li et al., 2021b; Luo et al., 2021; Martínez et al., 2020).

#### 2.3.1. HMF electrooxidation

The electrochemical oxidation of HMF is an excellent choice to substitute OER, which is a thermodynamically more suitable process and thus allows energy-saving hydrogen production. For instance, using the  $\text{MoO}_2\text{-FeP@C}||\text{MoO}_2\text{-FeP@C}$  as both the anode and the cathode, Yang et al. noticed that the addition of 0.01 M HMF in the 1.0 M KOH solution significantly reduced the required cell voltage to deliver 10  $\text{mA cm}^{-2}$  (1.486 vs. 1.592 V) (Yang et al., 2020). Moreover, this hybrid system has substantial economic importance because HMF is a vital platform chemical, and it can be upgraded to many value-added compounds such as 5-formylfuran (DFF), the 2-formyl-5-furan carboxylic acid (FFCA), the 5-hydroxymethyl-2-furan carboxylic acid (HMFC), and 2,5-furan dicarboxylic acid (FDCA). Among these oxidation products, FDCA is an essential substrate in the polymer industry and a vital precursor to produce fine chemicals (Xie et al., 2021); hence most studies focus on selective FDCA production.

Figure 2d shows the oxidation mechanism of HMF, and the formation of FDCA from HMF can follow two pathways, namely the DFF-pathway and the HMFC-pathway. Recent studies suggest that the reaction mechanism heavily relies on electrocatalysts and the applied potential. For example, Deng et al. found that the oxidation products on electrodeposited  $\text{CoO}_x\text{H}_y$  could be tuned between HMFC and FDCA by regulating the applied potential. The higher potential induced the gen-

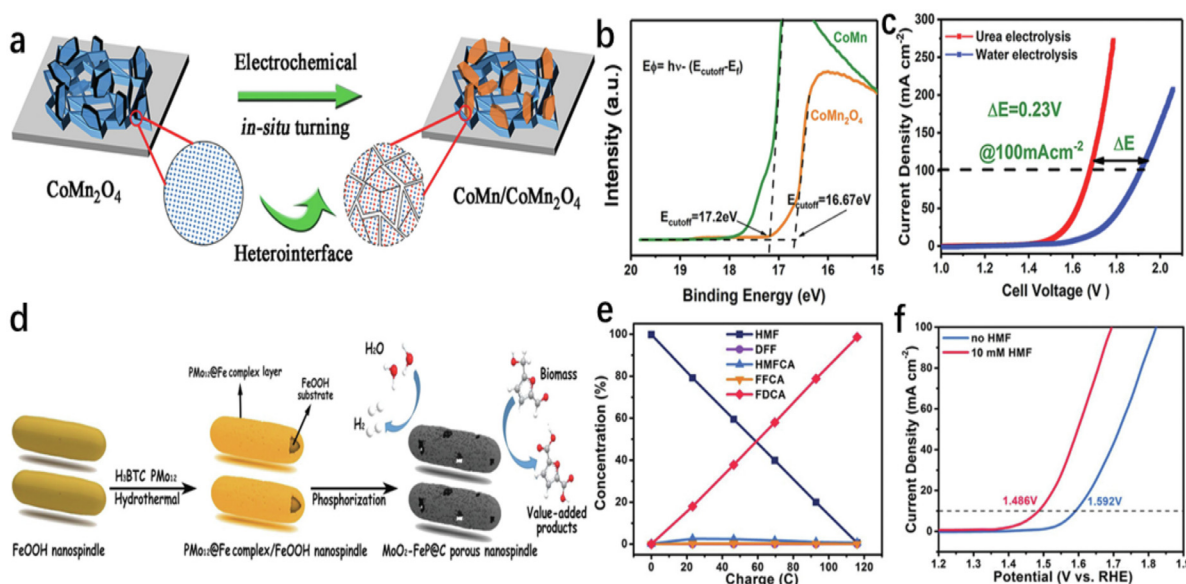


**Figure 4.** (a) Scheme of the preparation of CoMn/CoMn<sub>2</sub>O<sub>4</sub>. (b) Ultraviolet photoelectron spectroscopy analysis of CoMn<sub>2</sub>O<sub>4</sub> and CoMn. (c) Polarization curves for the urea assisted water electrolysis and PWE with CoMn<sub>2</sub>O<sub>4</sub> as the bifunctional catalyst (Wang et al., 2020). Reprinted with permission from Copyright 2020, Wiley-VCH. (d) Scheme of the preparation of the MoO<sub>2</sub>-FeP@C. (e) Conversion changes of HMF during the HMF electrooxidation process. (f) Polarization curves for HMF assisted water splitting and PWE with MoO<sub>2</sub>-FeP@C as the bifunctional catalyst (Yang et al., 2020). Reprinted with permission from Copyright 2020, Wiley-VCH.

eration of Co<sup>4+</sup>. Compared with the sluggish chemical oxidant Co<sup>3+</sup>, the Co<sup>4+</sup> allows the dehydrogenation of hydroxyl groups with obviously enhanced reaction kinetics, thus leading to the formation of FDCA (Deng et al., 2021b). A similar study reported by Xie and coworkers also suggests the potential-dependent selectivity on a CoFe@NiFe catalyst. They found that HMF electrooxidation mainly followed the HMFCA-pathway at low potentials (e.g., 1.34 V). At the same time, DFF-pathway was the primary oxidation process at high potentials (e.g., 1.5 V) (Xie et al., 2021). Density functional theory (DFT) calculations indicate that the PDSs of the two pathways are different on the NiOOH surface (Figure 2e). The first step in the HMFCA-pathway and the final step in the DFF-pathway are the PDSs for each route with the activation energies of 1.2 and 0.8 eV, respectively (Lu et al., 2021). Recently, a group of highly selective catalysts have been designed, such as CoFe@NiFe (Xie et al., 2021), (FeCrCoNiCu)<sub>3</sub>O<sub>4</sub> nanosheets (Wang et al., 2021b), LiMnBPO (Menezes et al., 2021), and MoO<sub>2</sub>-FeP (Yang et al., 2020). Further studies are encouraged to explore novel catalysts allowing the simultaneous production of H<sub>2</sub> and FDCA at low overpotentials and to identify the oxidation mechanism with theoretical and in situ experimental tools.

### 2.3.2. Small molecule alcohol electrooxidation

Small molecule alcohols (e.g., methanol, ethanol) can be produced as targets or byproducts in biomass valorization reactions. The electrooxidation of these small molecule alcohols is a great candidate to substitute OER for energy-saving hydrogen production. Sheng et al. assembled a hybrid ethanol-water electrolyzer with Co-S-P/CC as the cathode and the anode, which only required 1.63 V to attain 10 mA cm<sup>-2</sup>, outperforming the PWE (1.77 V) (Sheng et al., 2020). Alcohol compounds undergo complete or partial oxidation in the electrochemical process, and partial oxidation leads to value-added compounds (Yin et al., 2021). For methanol, the main oxidative products are H<sub>2</sub>O and CO<sub>2</sub>, which involves a six-electron transfer process (Figure 2f) (Li et al., 2021b; Ozoemena, 2016). The electrochemical oxidation of methanol consists of the dehydrogenation of methanol, the stripping, and the oxidation of carbon-bearing species.

Increasing the carbon chain, the electrooxidation reaction pathways become more difficult because of the solid C-C bonds. Nevertheless, ethanol possesses many critical advantages over methanol, including

low toxicity, ease of production and transportation, and higher energy density (8.0 vs. 6.1 kW h kg<sup>-1</sup>) (Yang et al., 2021b). In acidic media, the primary oxidation products of ethanol are CO<sub>2</sub>, CH<sub>3</sub>CHO, and CH<sub>3</sub>COOH. As depicted in Figure 2g, the complete oxidation of ethanol to CO<sub>2</sub> follows a 12-electron pathway. It needs to destroy the solid C-C bon. The partial oxidation may form CH<sub>3</sub>COOH and CH<sub>3</sub>CHO via 4-electron and 2-electron processes, respectively (Ozoemena, 2016). It should be noticed that the applied potential profoundly influences the oxidation mechanism of ethanol. Based on the in situ attenuated total reflection surface-enhanced infrared absorption spectroscopy results, Yang et al. suggested that the adsorbed acyl species (CH<sub>3</sub>CO<sub>ad</sub>) were formed at the lower potential (< -0.1 V), which were further oxidized via a C1 pathway to CO<sub>ad</sub> and CH<sub>x</sub> and eventually to CO<sub>2</sub> (at low potentials) or a C2 pathway to generate CH<sub>3</sub>COO<sup>-</sup> (at high potentials) (Yang et al., 2014). Hence, controlling the experimental conditions (pH value, applied potential) and electrocatalysts plays a critical role in regulating the reaction selectivity and enhancing the reaction efficiency to obtain value-added chemicals and hydrogen within alcohol hybridized water splitting systems.

## 3. Electrocatalysts for alternative oxidation reactions hybridized water electrolysis

Electrocatalysts can reduce the reaction energy barrier, facilitate reaction kinetics, regulate reaction selectivity, and improve energy utilization efficiency (Chen et al., 2020a). Therefore, many efforts have been made to design efficient catalysts for the aforementioned hybrid water electrolysis (Table 1), aiming to reduce the energy consumption for hydrogen production and gain favorable value-added oxidation products. This section introduces high-performance electrocatalysts applied in alternative oxidation reactions coupled with water splitting systems, and the catalyst properties-performance relationship is emphasized.

### 3.1. Metals and alloys

Metals and alloys, especially noble metals (alloys), are excellent electrocatalysts for both cathodic reaction (HER) and anodic reactions (oxidation of methanol, ethanol, and formic acid) due to their high electrocatalytic activities and good durability. Noble metals (e.g., Pt, Ir,

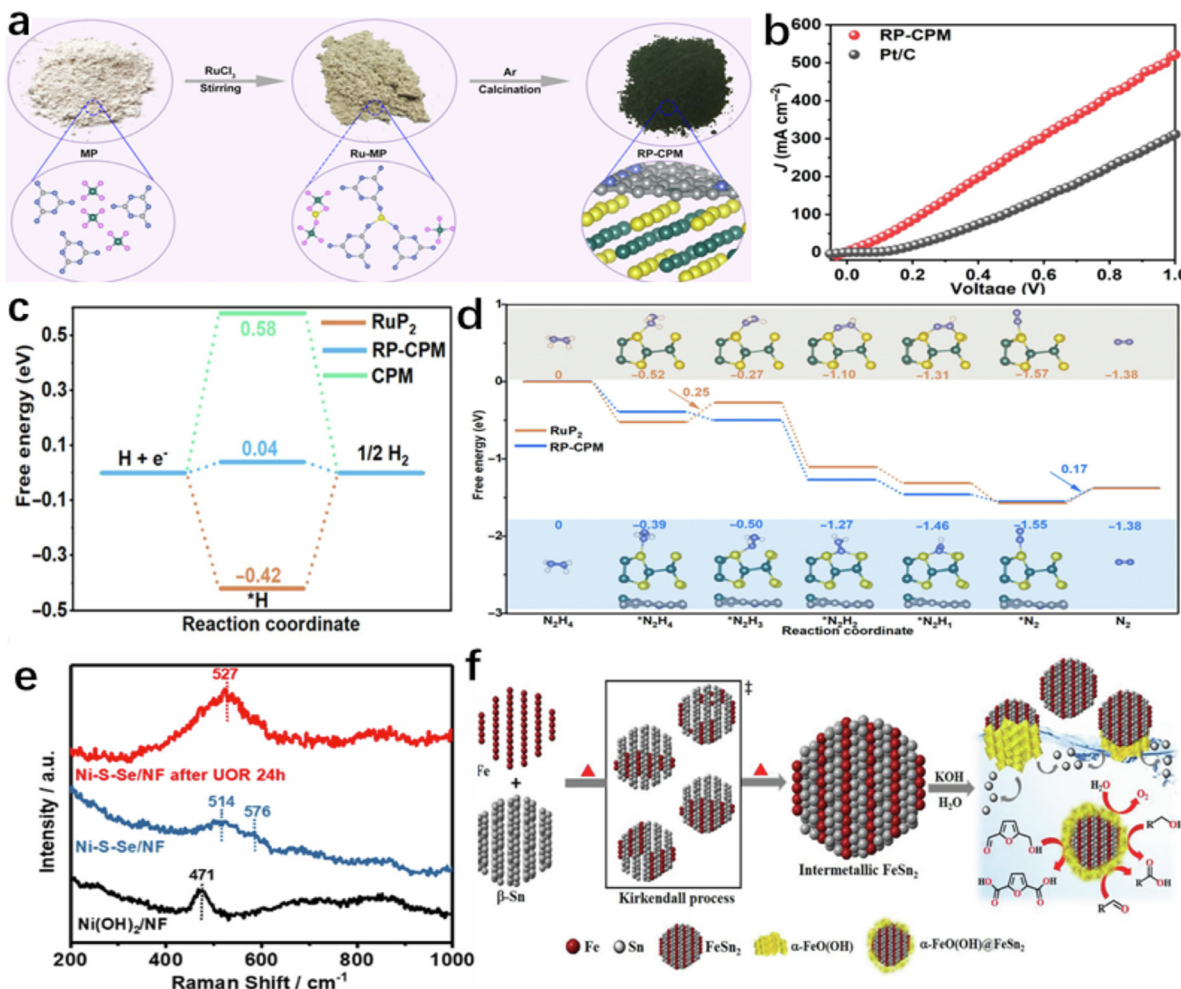


**Figure 5.** (a) Scheme of the formation process for RP-CPM. (b) Polarization curves of RP-CPM||RP-CPM and commercial Pt/C||Pt/C couples for hydrazine-assisted water splitting. (c) Free energy diagrams of HER for CPM, RP-CPM, and RuP<sub>2</sub>. (d) Free energy diagrams of HzOR for RP-CPM (down) and RuP<sub>2</sub> (up) (Li et al., 2020). Reprinted with permission from Copyright 2020, American Association for the Advancement of Science. (e) Raman spectra of pristine Ni-S-Se/NF, Ni(OH)<sub>2</sub>/NF, and Ni-S-Se/NF after urea electrooxidation (Chen et al., 2021a). Reprinted with permission from Copyright 2021, Elsevier. (f) Scheme of the formation of intermetallic FeSn<sub>2</sub> and the in situ electrochemical evolution of highly active crystalline  $\alpha$ -FeO(OH)@FeSn<sub>2</sub> to catalyze OER and organic oxidations (Chakraborty et al., 2020). Reprinted with permission from Copyright 2020, Wiley-VCH.

and Pd) have been widely used to catalyze alcohol oxidation (Bai et al., 2019; Park et al., 2020). To improve the catalytic performance and cost-effectiveness of noble metal-based catalysts, three strategies are widely suggested: alloying noble metals with another metal, nanostructure/composition regulation (Sun et al., 2020), and regulating the surface chemistry of catalysts (exposing desirable crystallographic facets) (Li et al., 2021a). Yin et al. recently reported bifunctional 1 nm PtIr nanowires (NWs, Figures 3a-b) for the electrosynthesis of high-purity hydrogen at the cathode and 1,1-dimethoxyethane (DEE) at the anode from the ethanol-assisted water electrolyzer. The PtIr NWs could improve the activation of C-H and O-H bonds in ethanol molecules, promoting the generation of acetaldehyde intermediate and the final DEE. Compared with the Pt NWs, the alloy required a lower voltage (0.61 vs. 0.85 V) to reach 10  $\text{mA cm}^{-2}$  in a two-electrode electrolyzer (Figures 3c-d). In addition, this study also showed that the Faraday efficiency (FE) of DEE depended on the property of acids, and the highest FE of DEE reached 85% at 10  $\text{mA cm}^{-2}$  in perchloric acid ethanol solution (Figure 3e). The difference of FE in diverse acids might be due to their acidity in an ethanol solution, which determines the acetylation rate and intensity (Yin et al., 2021). Alloying noble metals with 3d transition metals can significantly reduce the catalyst cost and enhance the catalytic performance. Du et al. found that the bifunctional

Ni@Pd-Ni alloy NW significantly outperformed the Ni NW for the oxidation of N<sub>2</sub>H<sub>4</sub>. Compared with PWE, the alloy NW took a lower cell voltage of 0.58 V to drive a current density of 15  $\text{mA cm}^{-2}$  in the N<sub>2</sub>H<sub>4</sub>-containing electrolyzer (reduced by 72.26 % than that in PWE) (Du et al., 2019).

Developing noble metal-free catalysts is gaining growing scientific attention. Low-cost transition metal-based single atom (SA) catalysts (e.g., FeSA/CNT (Zhang et al., 2021a)) and alloys (e.g., NiCu (Sun et al., 2018), NiFe (Cao et al., 2020), and NiZn (Feng et al., 2020)) have exhibited good electrocatalytic performance for hybrid water electrolysis systems. For example, Zhang and coworkers designed a series of MSA/CNT (M = Fe, Co, Ni) with an M-N<sub>4</sub>-C configuration via a pyrolysis process. Among the three SA catalysts, FeSA/CNT showed the most robust interaction with N<sub>2</sub>H<sub>4</sub> (-1.47 eV), which could benefit HzOR as the adsorption of N<sub>2</sub>H<sub>4</sub> is the first step of the reaction and the stable adsorption of  $^*\text{N}_2\text{H}_4$  on the catalyst facilitated the reaction (Figure 3f). Such DFT results were consistent with the highest current density (12,493  $\text{A g}_{\text{Fe}}^{-1}$ ) of FeSA/CNT for the HzOR (Figure 3g). Compared with FeSA/CN and CoSA/CNT, NiSA/CNT exhibited a more considerable uphill energy barrier (1.14 eV) for the first dehydrogenation step, resulting in the lowest HzOR activity (Figure 3h) (Zhang et al., 2021a). Accordingly, developing high-efficiency noble metal-free single atom/alloy catalysts is a

**Table 1**

A summary of catalytic performance of typical catalysts for the alternative oxidation reactions.

Catalyst <sup>a</sup>	Electrolyte	Performance	Ref.
Ni <sub>2</sub> P/Ni <sub>0.96</sub> S/NF  Ni <sub>2</sub> P/Ni <sub>0.96</sub> S/NF	1.0 M KOH + 0.5 M urea 1.0 M KOH	100 mA cm <sup>-2</sup> @1.453 V 100 mA cm <sup>-2</sup> @1.639 V	(He et al., 2020)
NP-Ni <sub>0.70</sub> Fe <sub>0.30</sub>   NP-Ni <sub>0.70</sub> Fe <sub>0.30</sub>	1.0 M KOH + 0.33 M urea 1.0 M KOH	10 mA cm <sup>-2</sup> @1.55 V 10 mA cm <sup>-2</sup> @1.68 V	(Cao et al., 2020)
Ni-S-Se/NF  Ni-S-Se/NF	1.0 M KOH + 0.5 M urea 1.0 M KOH	10 mA cm <sup>-2</sup> @1.47 V 10 mA cm <sup>-2</sup> @1.57 V	(Chen et al., 2021a)
Ni@Pd–Ni alloy NAs  Ni@Pd–Ni alloy NAs	1.0 M KOH + 0.02 M hydrazine 1.0 M KOH	15 mA cm <sup>-2</sup> @0.63 V 15 mA cm <sup>-2</sup> @1.97 V	(Du et al., 2019)
Ni-15 at.% Zn/rGO  Ni-15 at.% Zn/rGO	1.0 M KOH + 0.5 M hydrazine 1.0 M KOH	100 mA cm <sup>-2</sup> @0.418 V 100 mA cm <sup>-2</sup> @2.458 V	(Feng et al., 2020)
RP-CPM  RP-CPM	1.0 M KOH + 0.3 M hydrazine 1.0 M KOH	10 mA cm <sup>-2</sup> @0.023 V 10 mA cm <sup>-2</sup> @2.439 V	(Li et al., 2020)
Co-S-P/CC  Co-S-P/CC	1.0 M KOH + 1.0 M ethanol 1.0 M KOH	10 mA cm <sup>-2</sup> @1.63 V 10 mA cm <sup>-2</sup> @1.77 V	(Sheng et al., 2020)
CoS <sub>2</sub> -MoS <sub>2</sub>   CoNi-PHNs	1.0 M KOH + 1.0 M ethanol 1.0 M KOH	~10 mA cm <sup>-2</sup> @1.57 V ~10 mA cm <sup>-2</sup> @1.77 V	(Wang et al., 2019a)
Au@Pt <sub>0.077</sub> Au UFNWs  Au@Pt <sub>0.077</sub> Au UFNWs	0.5 M H <sub>2</sub> SO <sub>4</sub> + 1 M formic acid 0.5 M H <sub>2</sub> SO <sub>4</sub>	10 mA cm <sup>-2</sup> @0.51 V 10 mA cm <sup>-2</sup> @1.49 V	(Xue et al., 2022)
MoO <sub>2</sub> -FeP@C  MoO <sub>2</sub> -FeP@C	1 M KOH + 0.01 M 5-hydroxymethylfurfural 1.0 M KOH	10 mA cm <sup>-2</sup> @1.486 V 10 mA cm <sup>-2</sup> @1.592 V	(Yang et al., 2020)
CNTs@Co/CoP  CNTs@Co/CoP	1 M KOH + 0.5 M glucose 1 M KOH	10 mA cm <sup>-2</sup> @1.42 V 10 mA cm <sup>-2</sup> @1.74 V	(Zhang et al., 2021c)
h-NiSe/CNTs  h-NiSe/CNTs	1.0 M KOH + 1.0 M methanol 1.0 M KOH	H <sub>2</sub> generation rate ~44.5 × 10 <sup>-8</sup> mol s <sup>-1</sup> <sup>b</sup> H <sub>2</sub> generation rate ~7.19 × 10 <sup>-8</sup> mol s <sup>-1</sup>	(Zhao et al., 2020a)

<sup>a</sup> Cathode||Anode.<sup>b</sup> Measured at 1.62 V vs. RHE.

sensible way further to reduce the running cost of hybrid water electrolysis systems.

### 3.2. Metal oxides and hydroxides

Electrocatalysts based on transition metal (hydr)oxides attract growing attention due to their flexible chemical compositions/nanostructures, high catalytic activity, and low cost. Ni/Co/Fe-based metal (hydr)oxides have shown efficient electrocatalytic performance for the electrooxidation mentioned above reactions (Deng et al., 2021a; Taitt et al., 2018). For example, Xie et al. recently reported a hierarchically layered double hydroxide (CoFe@NiFe) for the selective oxidation of HMF. Coupled with HER, the HMF assisted water splitting attained 38 mA cm<sup>-2</sup> at a low potential of 1.40 V and showed a high selectivity of 100% to form the desirable FDCA and a Faraday efficiency of about 100% with a high hydrogen generation efficiency of 901 μmol cm<sup>-2</sup> (Xie et al., 2021).

To improve the catalytic efficiency and reaction selectivity, it is necessary to regulate catalysts' nanostructure rationally and surface chemistry. For ethanol oxidation, the diverse chemical bonds and functional groups of ethanol often lead to unsatisfied catalytic efficiency and selectivity. In addition, large channels are required to transport molecules/ions due to the relatively large size and viscosity of ethanol molecules. Wang et al. suggested that the ultrathin perforated CoNi hydroxide nanosheets could meet these requirements. In their designed perforated CoNi hydroxide nanosheets, the ultrathin structure guaranteed the ultrahigh exposure of electroactive surface area and quick charge/mass transportation. Additionally, the interaction among various metal atoms modulated the electron density near the electroactive sites to form reaction intermediates' more appropriate adsorption/desorption behavior (Wang et al., 2019a). Their results indicate that controllable design of nanostructure can realize synergistic modulation of geometric and electronic properties and thus achieve efficient electrooxidation.

Constructing heterostructures is another efficient way to attain high-performance electrocatalysts, increasing the active sites and manipu-

lating the intrinsic activity via chemical coupling effects (Chen et al., 2020b). Wang et al. prepared a CoMn/CoMn<sub>2</sub>O<sub>4</sub> Schottky catalyst via an electrochemical tuning treatment (Figure 4a). The ultraviolet photo-electron spectroscopy analysis suggested that CoMn possessed a lower work function value than the CoMn<sub>2</sub>O<sub>4</sub> (4 vs. 4.53 eV) (Figure 4b), which met the need for generating the Schottky barrier energy band. The Schottky barrier would lead to electron redistribution and band bending at the interface, which allowed the spontaneous electron transfer from CoMn to CoMn<sub>2</sub>O<sub>4</sub> until the work function reached equilibrium. The self-driven charge transfer behavior would facilitate the decomposition of urea and water and the absorption of reactants. Better than CoMn<sub>2</sub>O<sub>4</sub>, the bifunctional CoMn/CoMn<sub>2</sub>O<sub>4</sub> could attain 10 mA cm<sup>-2</sup> at 1.51 V in the full urea-assisted energy-saving electrolysis (Figure 4c) (Wang et al., 2020). Considering the high electroactivity of metal phosphides, Yang et al. developed a carbon-encapsulated MoO<sub>2</sub>-FeP heterojunction (MoO<sub>2</sub>-FeP@C) via a two-step method (Figure 4d). Compared with MoO<sub>2</sub> and FeP, MoO<sub>2</sub>-FeP@C showed a higher HMF conversion (99.4%), a better FDCA selectivity (98.6%), and a higher FE (97.8%) (Figure 4e). The HMF coupled water electrolysis could save 106 mV from achieving 10 mA cm<sup>-2</sup> than PWE in 1.0 M KOH with 10 mM HMF. (Figure 4f) (Yang et al., 2020).

### 3.3. Metal chalcogenides and pnictides

The high electrocatalytic activity, suitable metallic property, and increased reaction selectivity of metal chalcogenides and pnictides make them suitable catalysts for electrochemical oxidation reactions (Zhao et al., 2020a). For example, Li et al. reported a high-performance bifunctional partially exposed RuP<sub>2</sub> nanoparticle-decorated carbon porous microsheets (RP-CPM) (Figure 5a), which reached 10 and 522 mA cm<sup>-2</sup> at cell voltages of 23 mV and 1.0 V in 1.0 M KOH/0.5 M N<sub>2</sub>H<sub>4</sub> electrolyte, respectively (Figure 5b). In-depth calculations revealed the nobility of the partial exposure of RuP<sub>2</sub> in the heterostructure. The C atoms exhibited a favorable HER activity (Figure 5c), while the exposed surface Ru atoms were the electroactive sites for HzOR (Figure 5d) (Li et al., 2020). Beyond the noble metal phosphide/carbon hybrids, many

low-cost heterostructures also exhibit suitable bifunctional activities for hybrid water electrolysis, such as Cu<sub>2</sub>Se/Co<sub>3</sub>Se<sub>4</sub> (Zhao et al., 2021a), h-NiSe/CNTs (Zhao et al., 2020a), N doped NiS/NiS<sub>2</sub> (Liu et al., 2020b), Co<sub>3</sub>S<sub>4</sub>-NSs/Ni-F (Ding et al., 2021), and Ni<sub>2</sub>P/Ni<sub>0.96</sub>S (He et al., 2020).

The chemical composition of catalysts dominates the catalytic performance via regulating the electronic structure and surface chemistry. In this context, designing binary-nonmetal compounds and doping are two efficient strategies. Sheng and co-authors designed bifunctional Co-S-P nanosheet arrays for HER and ethanol electrooxidation. Benefiting from the favorable thermodynamics and kinetics of ethanol electrooxidation over OER, the potential needed for the ethanol hybrid water splitting was 1.63 V at 10 mA cm<sup>-2</sup> in 1.0 M KOH with 1.0 M ethanol, which was 0.14 V lower than that for PWE (Sheng et al., 2020). In another study, Chen et al. reported an amorphous bifunctional Ni-S-Se catalyst for urea hybridized water splitting. They found that the in situ generated amorphous NiOOH acted as the real electroactive sites for urea oxidation, as evidenced by the Raman spectra (Figure 5e). The urea-coupled water electrolyzer assembled by the Ni-S-Se electrodes attained 10 mA cm<sup>-2</sup> at 1.47 V in 1 M KOH with 0.5 M urea (Chen et al., 2021a). It should be noticed that the surface self-reconstruction of transition metal-based catalysts profoundly influences catalytic performance. Chakraborty et al. suggested that the superior activity of FeSn<sub>2</sub> resulted from the in-situ generation of the  $\alpha$ -FeO(OH)@FeSn<sub>2</sub> hybrid under the oxidation conditions, and  $\alpha$ -FeO(OH) acted as the active site. At the same time, FeSn<sub>2</sub> remained the conductive core (Figure 5f) (Chakraborty et al., 2020).

Rationally incorporating foreign elements can enhance the catalytic performance of nanomaterials. The foreign dopants can diminish the agglomeration, provide more electroactive sites, regulate the crystal structure, and modulate the electronic structure (Chen et al., 2020b). Liu et al. found that the N-doping could enlarge the surface area, induce interfacial coupling and synergistic effect between NiS<sub>2</sub> and NiS, and thus enhance the UOR performance (Liu et al., 2020b). Furthermore, Liu and coworkers developed a P, W co-doped Co<sub>3</sub>N via a hydrothermal method followed by annealing treatment. For the oxidation of hydrazine, the P, W co-doping could reduce the free energy of PDS and thus lead to an enhanced electrocatalytic activity (Liu et al., 2020c).

#### 4. Conclusions and perspectives

Developing hybrid water splitting for energy-saving hydrogen production is significant in advancing the global sustainable energy scheme. Herein, the fundamentals of typical electrochemical oxidation reactions (e.g., UOR, HzOR, biomass oxidation) are firstly presented. Then, recent achievements in electrocatalysts for hybrid water splitting are analyzed, and many essential catalyst design strategies are outlined and the underlying catalyst structure-performance relationship.

Some critical aspects require further exploration to realize the large-scale and commercial application of hybrid water electrolysis. Firstly, applying DFT calculations-machine learning strategy for electrocatalyst discovery would significantly accelerate the design of novel high-efficiency catalysts and enable a deeper understanding of the underlying correlation between the catalyst structure and their catalytic performance. Secondly, integrating *in situ* techniques (e.g., Raman spectroscopy, X-ray diffraction spectroscopy, and X-ray absorption spectroscopy) and analytical methods (e.g., inductively coupled plasma mass spectrometry) is necessary to monitor the reaction intermediates and to explore the dynamic structure self-reconstruction of catalysts during the electrochemical reactions, which will benefit the understanding of the electrochemical oxidation process as well as high-performance catalyst design. Thirdly, developing bifunctional catalysts based on earth-abundant elements for hybrid water splitting is highly advisable for cost reduction, simplification, and practical applications. Fourthly, it is essential to develop new oxidation reactions, especially the electrooxidation of biomass and pollutants (e.g., sulfides, halides), to harvest hydrogen and critical value-added products or simultaneously degrade the

hazards with low energy consumption. In this context, membrane-based practical systems are required to separate the anode and cathode products and select the membrane governed by the applied electrolyte. At last, for the large-scale and commercial application of hybrid water electrolysis, it is necessary to integrate the electrolyzer with a solar system to minimize the energy cost further.

#### Declaration of interests

The authors declare that they have no known competing financial interests or personal relationships that could have appeared to influence the work reported in this paper.

#### Acknowledgments

This work is supported by the Australian Research Council (ARC) Future Fellowship (FT160100195). Dr. Wei Wei acknowledges the support of the Australian Research Council (ARC) through project DE220100530. Mr. Zhiping Chen also thanks to the support from China Scholarship Council (CSC).

#### Supplementary materials

Supplementary material associated with this article can be found, in the online version, at doi:10.1016/j.horiz.2021.100002.

#### References

- Ali, A., Shen, P.K., 2020. Nonprecious metal's graphene-supported electrocatalysts for hydrogen evolution reaction: Fundamentals to applications. *Carbon Energy* 2 (1), 99–121.
- Anantharaj, S., Aravindan, V., 2020. Developments and perspectives in 3d transition-metal based electrocatalysts for neutral and near-neutral water electrolysis. *Adv. Energy Mater.* 10 (1), 1902666.
- Bai, J., Liu, D., Yang, J., Chen, Y., 2019. Nanocatalysts for electrocatalytic oxidation of ethanol. *ChemSusChem* 12 (10), 2117–2132.
- Bender, M.T., Yuan, X., Choi, K.S., 2020. Alcohol oxidation as alternative anode reactions paired with (photo)electrochemical fuel production reactions. *Nat. Commun.* 11 (1), 4594.
- Berger, A., Segalman, R.A., Newman, J., 2014. Material requirements for membrane separators in a water-splitting photoelectrochemical cell. *Energy Environ. Sci.* 7 (4), 1468–1476.
- Cao, Z., Zhou, T., Ma, X., Shen, Y., Deng, Q., Zhang, W., Zhao, Y., 2020. Hydrogen production from urea sewage on NiFe-based porous electrocatalysts. *ACS Sustainable Chem. Eng.* 8 (29), 11007–11015.
- Chakraborty, B., Beltrán-Suito, R., Hausmann, J.N., Garai, S., Driess, M., Menezes, P.W., 2020. Enabling iron-based highly effective electrochemical water-splitting and selective oxygenation of organic substrates through *in situ* surface modification of intermetallic iron stannide precatalyst. *Adv. Energy Mater.* 10 (30), 2001377.
- Chen, N., Du, Y.-X., Zhang, G., Lu, W.-T., Cao, F.-F., 2021a. Amorphous nickel sulfoselenide for efficient electrochemical urea-assisted hydrogen production in alkaline media. *Nano Energy* 81, 105605.
- Chen, Z., Duan, X., Wei, W., Wang, S., Ni, B.-J., 2019. Recent advances in transition metal-based electrocatalysts for alkaline hydrogen evolution. *J. Mater. Chem. A* 7 (25), 14971–15005.
- Chen, Z., Duan, X., Wei, W., Wang, S., Ni, B.-J., 2020a. Electrocatalysts for acidic oxygen evolution reaction: Achievements and perspectives. *Nano Energy* 78, 105392.
- Chen, Z., Duan, X., Wei, W., Wang, S., Zhang, Z., Ni, B.-J., 2020b. Boride-based electrocatalysts: Emerging candidates for water splitting. *Nano Res* 13 (2), 293–314.
- Chen, Z., Wei, W., Ni, B.-J., 2021b. Cost-effective catalysts for renewable hydrogen production via electrochemical water splitting: Recent advances. *Curr. Opin. Green Sustain. Chem.* 27, 100398.
- Chen, Z., Zheng, R., Graś, M., Wei, W., Lota, G., Chen, H., Ni, B.-J., 2021c. Tuning electronic property and surface reconstruction of amorphous iron borides via W-P co-doping for highly efficient oxygen evolution. *Appl. Catal. B* 288, 120037.
- Chen, Z., Zou, W., Zheng, R., Wei, W., Wei, W., Ni, B.-J., Chen, H., 2021d. Synergistic recycling and conversion of spent Li-ion battery leachate into highly efficient oxygen evolution catalysts. *Green Chem* 23, 6538–6547.
- Deng, C., Wu, K.H., Lu, X., Cheong, S., Tilley, R.D., Chiang, C.L., Lin, Y.C., Lin, Y.G., Yan, W., Scott, J., Amal, R., Wang, D.W., 2021a. Ligand-promoted cooperative electrochemical oxidation of bio-alcohol on distorted cobalt hydroxides for bio-hydrogen extraction. *ChemSusChem* 14, 2612.
- Deng, X., Xu, G.-Y., Zhang, Y.-J., Wang, L., Zhang, J., Li, J.-F., Fu, X.-Z., Luo, J.-L., 2021b. Understanding the roles of electrogenerated Co<sup>3+</sup> and Co<sup>4+</sup> in selectivity-tuned 5-hydroxymethylfurfural oxidation. *Angew. Chem. Int. Ed.* doi:10.1002/ange.202108955.

- Ding, Y., Xue, Q., Hong, Q.-L., Li, F.-M., Jiang, Y.-C., Li, S.-N., Chen, Y., 2021. Hydrogen and potassium acetate co-production from electrochemical reforming of ethanol at ultrathin cobalt sulfide nanosheets on nickel foam. *ACS Appl. Mater. Interfaces* 13 (3), 4026–4033.
- Du, L., Sun, Y., You, B., 2020. Hybrid water electrolysis: Replacing oxygen evolution reaction for energy-efficient hydrogen production and beyond. *Materials Reports: Energy* 1 (1), 100004.
- Du, M., Sun, H., Li, J., Ye, X., Yue, F., Yang, J., Liu, Y., Guo, F., 2019. Integrative Ni@Pd-Ni alloy nanowire array electrocatalysts boost hydrazine oxidation kinetics. *ChemElectroChem* 6 (22), 5581–5587.
- Fan, L., Liu, B., Liu, X., Senthilkumar, N., Wang, G., Wen, Z., 2020. Recent progress in electrocatalytic glycerol oxidation. *Energy Technol* 9 (2), 2000804.
- Feng, Z., Zhang, H., Gao, B., Lu, P., Li, D., Xing, P., 2020. Ni-Zn nanosheet anchored on rGO as a bifunctional electrocatalyst for efficient alkaline water-to-hydrogen conversion via hydrazine electrolysis. *Int. J. Hydrogen Energy* 45 (38), 19335–19343.
- Gnana Kumar, G., Farithkhan, A., Manthiram, A., 2020. Direct urea fuel cells: Recent progress and critical challenges of urea oxidation electrocatalysis. *Adv. Energy Sustain. Res.* 1 (1), 2000015.
- Gomes, J.F., Tremiliosi-Filho, G., 2011. Spectroscopic studies of the glycerol electro-oxidation on polycrystalline Au and Pt surfaces in acidic and alkaline media. *Electrocatalysis* 2 (2), 96–105.
- Han, W.K., Li, X.P., Lu, L.N., Ouyang, T., Xiao, K., Liu, Z.Q., 2020. Partial S substitution activates NiMoO<sub>4</sub> for efficient and stable electrocatalytic urea oxidation. *Chem. Commun.* 56 (75), 11038–11041.
- He, M., Feng, C., Liao, T., Hu, S., Wu, H., Sun, Z., 2020. Low-cost Ni<sub>2</sub>P/Ni<sub>0.96</sub>S heterostructured bifunctional electrocatalyst toward highly efficient overall urea-water electrolysis. *ACS Appl. Mater. Interfaces* 12 (2), 2225–2233.
- Hu, X., Zhu, J., Li, J., Wu, Q., 2020. Urea electrooxidation: Current development and understanding of Ni-based catalysts. *ChemElectroChem* 7 (15), 3211–3228.
- Huang, C., Huang, Y., Liu, C., Yu, Y., Zhang, B., 2019. Integrating hydrogen production with aqueous selective semi-dehydrogenation of tetrahydroisoquinolines over a Ni<sub>2</sub>P bifunctional electrode. *Angew. Chem. Int. Ed.* 58 (35), 12014–12017.
- Li, C., Chen, X., Zhang, L., Yan, S., Sharma, A., Zhao, B., Kumbhar, A., Zhou, G., Fang, J., 2021a. Synthesis of core@shell Cu-Ni@Pt-Cu nano-octahedra and their improved MOR activity. *Angew. Chem. Int. Ed.* 60 (14), 7675–7680.
- Li, Y., Dang, Z., Gao, P., 2021b. High-efficiency electrolysis of biomass and its derivatives: Advances in anodic oxidation reaction mechanism and transition metal-based electrocatalysts. *Nano Select* 2 (5), 847–864.
- Li, Y., Zhang, J., Liu, Y., Qian, Q., Li, Z., Zhu, Y., Zhang, G., 2020. Partially exposed RuP<sub>2</sub> surface in hybrid structure endows its bifunctionality for hydrazine oxidation and hydrogen evolution catalysis. *Sci. Adv.* 6 (44), eabb4197.
- Liao, G., Gong, Y., Zhang, L., Gao, H., Yang, G.-J., Fang, B., 2019. Semiconductor polymeric graphitic carbon nitride photocatalysts: the “holy grail” for the photocatalytic hydrogen evolution reaction under visible light. *Energy Environ. Sci.* 12 (7), 2080–2147.
- Liu, H., Liu, Y., Li, M., Liu, X., Luo, J., 2020a. Transition-metal-based electrocatalysts for hydrazine-assisted hydrogen production. *Mater. Today Adv.* 7, 100083.
- Liu, H., Liu, Z., Wang, F., Feng, L., 2020b. Efficient catalysis of N doped NiS/NiS<sub>2</sub> heterogeneous structure. *Chem. Eng. J.* 397, 125507.
- Liu, X., He, J., Zhao, S., Liu, Y., Zhao, Z., Luo, J., Hu, G., Sun, X., Ding, Y., 2018. Self-powered H<sub>2</sub> production with bifunctional hydrazine as sole consumable. *Nat. Commun.* 9 (1), 4365.
- Liu, Y., Zhang, J., Li, Y., Qian, Q., Li, Z., Zhu, Y., Zhang, G., 2020c. Manipulating dehydrogenation kinetics through dual-doping Co<sub>3</sub>N electrode enables highly efficient hydrazine oxidation assisting self-powered H<sub>2</sub> production. *Nat. Commun.* 11 (1), 1853.
- Lu, X., Wu, K.H., Zhang, B., Chen, J., Li, F., Su, B.J., Yan, P., Chen, J.M., Qi, W., 2021. Highly efficient electro-reforming of 5-hydroxymethylfurfural on vertically oriented nickel nanosheet/carbon hybrid catalysts: Structure-function relationships. *Angew. Chem. Int. Ed.* 60 (26), 14528–14535.
- Luo, H., Barrio, J., Sunny, N., Li, A., Steier, L., Shah, N., Stephens, I.E.L., Titirici, M.M., 2021. Progress and perspectives in photo- and electrochemical-oxidation of biomass for sustainable chemicals and hydrogen production. *Adv. Energy Mater.*, 2101180.
- Martinez, N.P., Isaacs, M., Nanda, K.K., 2020. Paired electrolysis for simultaneous generation of synthetic fuels and chemicals. *New J. Chem.* 44 (15), 5617–5637.
- Menezes, P.W., Walter, C., Chakraborty, B., Hausmann, J.N., Zaharieva, I., Frick, A., Hauff, E., Dau, H., Driess, M., 2021. Combination of highly efficient electrocatalytic water oxidation with selective oxygenation of organic substrates using manganese borophosphates. *Adv. Mater.* 33 (9), 2004098.
- Ozoemena, K.I., 2016. Nanostructured platinum-free electrocatalysts in alkaline direct alcohol fuel cells: catalyst design, principles and applications. *RSC Adv* 6 (92), 89523–89550.
- Park, M., Gu, M., Kim, B.S., 2020. Tailorable electrocatalytic 5-hydroxymethylfurfural oxidation and H<sub>2</sub> production: Architecture-performance relationship in bifunctional multilayer electrodes. *ACS Nano* 14 (6), 6812–6822.
- Qian, G., Chen, J., Luo, L., Zhang, H., Chen, W., Gao, Z., Yin, S., Tsiaikaras, P., 2020. Novel bifunctional V<sub>2</sub>O<sub>3</sub> nanosheets coupled with N-doped-carbon encapsulated Ni heterostructure for enhanced electrocatalytic oxidation of urea-rich wastewater. *ACS Appl. Mater. Interfaces* 12 (34), 38061–38069.
- Sheng, S., Ye, K., Sha, L., Zhu, K., Gao, Y., Yan, J., Wang, G., Cao, D., 2020. Rational design of Co-S-P nanosheet arrays as bifunctional electrocatalysts for both ethanol oxidation reaction and hydrogen evolution reaction. *Inorg. Chem. Front.* 7 (22), 4498–4506.
- Song, J., Wei, C., Huang, Z.-F., Liu, C., Zeng, L., Wang, X., Xu, Z.J., 2020. A review on fundamentals for designing oxygen evolution electrocatalysts. *Chem. Soc. Rev.* 49 (7), 2196–2214.
- Sun, H.-Y., Xu, G.-R., Li, F.-M., Hong, Q.-L., Jin, P.-J., Chen, P., Chen, Y., 2020a. Hydrogen generation from ammonia electrolysis on bifunctional platinum nanocubes electrocatalysts. *J. Energy Chem.* 47, 234–240.
- Sun, Q., Wang, L., Shen, Y., Zhou, M., Ma, Y., Wang, Z., Zhao, C., 2018. Bifunctional copper-doped nickel catalysts enable energy-efficient hydrogen production via hydrazine oxidation and hydrogen evolution reduction. *ACS Sustainable Chem. Eng.* 6 (10), 12746–12754.
- Sun, X., Ding, R., 2020b. Recent progress with electrocatalysts for urea electrolysis in alkaline media for energy-saving hydrogen production. *Catal. Sci. Technol.* 10 (6), 1567–1581.
- Taitt, B.J., Nam, D.-H., Choi, K.-S., 2018. A comparative study of nickel, cobalt, and iron oxyhydroxide anodes for the electrochemical oxidation of 5-hydroxymethylfurfural to 5-furandicarboxylic acid. *ACS Catal* 9 (1), 660–670.
- Wang, C., Liu, H., Mao, Z., Yan, C., Shen, G., Wang, X., 2020. Bimetal schottky heterojunction boosting energy-saving hydrogen production from alkaline water via urea electrocatalysis. *Adv. Funct. Mater.* 30 (21), 2000556.
- Wang, F., Li, W., Wang, R., Guo, T., Sheng, H., Fu, H.-C., Stahl, S.S., Jin, S., 2021a. Modular electrochemical synthesis using a redox reservoir paired with independent half-reactions. *Joule* 5 (1), 149–165.
- Wang, S., Gu, K., Wang, D., Xie, C., Wang, T., Huang, G., Liu, Y., Zou, Y., Tao, L.I., 2021b. Defect-rich high-Entropy oxides nanosheets for efficient 5-hydroxymethylfurfural electrooxidation. *Angew. Chem. Int. Ed.* doi:10.1002/ange.202107390.
- Wang, W., Zhu, Y.B., Wen, Q., Wang, Y., Xia, J., Li, C., Chen, M.W., Liu, Y., Li, H., Wu, H.A., Zhai, T., 2019a. Modulation of molecular spatial distribution and chemisorption with perforated nanosheets for ethanol electro-oxidation. *Adv. Mater.* 31 (28), 1900528.
- Wang, X., Vasileff, A., Jiao, Y., Zheng, Y., Qiao, S.Z., 2019b. Electronic and structural engineering of carbon-based metal-free electrocatalysts for water splitting. *Adv. Mater.* 31 (13), 1803625.
- Wang, Z., Xu, L., Huang, F., Qu, L., Li, J., Owusu, K.A., Liu, Z., Lin, Z., Xiang, B., Liu, X., Zhao, K., Liao, X., Yang, W., Cheng, W.Y., Mai, L., 2019c. Copper-nickel nitride nanosheets as an efficient bifunctional catalysts for hydrazine-assisted electrolytic hydrogen production. *Adv. Energy Mater.* 9 (21), 1900390.
- Xie, Y., Zhou, Z., Yang, N., Zhao, G., 2021. An overall reaction integrated with highly selective oxidation of 5-hydroxymethylfurfural and efficient hydrogen evolution. *Adv. Funct. Mater.*, 2102886.
- Xu, J., Amorim, I., Li, Y., Li, J., Yu, Z., Zhang, B., Araujo, A., Zhang, N., Liu, L., 2020. Stable overall water splitting in an asymmetric acid/alkaline electrolyzer comprising a bipolar membrane sandwiched by bifunctional cobalt-nickel phosphide nanowire electrodes. *Carbon Energy* 2 (4), 646–655.
- Xue, Q., Bai, X.-Y., Zhao, Y., Li, Y.-N., Wang, T.-J., Sun, H.-Y., Li, F.-M., Chen, P., Jin, P., Yin, S.-B., 2022. Au core-PtAu alloy shell nanowires for formic acid electrolysis. *J. Energy Chem.* 65, 94–102.
- Yang, G., Jiao, Y., Yan, H., Xie, Y., Wu, A., Dong, X., Guo, D., Tian, C., Fu, H., 2020. Interfacial engineering of MoO<sub>2</sub>-FeP heterojunction for highly efficient hydrogen evolution coupled with biomass electrooxidation. *Adv. Mater.* 32 (17), 2000455.
- Yang, L., Liu, Z., Zhu, S., Feng, L., Xing, W., 2021a. Ni-based layered double hydroxide catalysts for oxygen evolution reaction. *Mater. Today Phys.* 16, 100292.
- Yang, X., Gao, Y., Zhao, Z., Tian, Y., Kong, X., Lei, X., Zhang, F., 2021b. Three-dimensional spherical composite of layered double hydroxides/carbon nanotube for ethanol electrocatalysis. *Appl. Clay Sci.* 202, 105964.
- Yang, Y.-Y., Ren, J., Li, Q.-X., Zhou, Z.-Y., Sun, S.-G., Cai, W.-B., 2014. Electrocatalysis of ethanol on a Pd electrode in alkaline media: An in situ attenuated total reflection surface-enhanced infrared absorption spectroscopy study. *ACS Catal* 4 (3), 798–803.
- Yin, K., Chao, Y., Lv, F., Tao, L., Zhang, W., Lu, S., Li, M., Zhang, Q., Gu, L., Li, H., Guo, S., 2021. One nanometer PtIr nanowires as high-efficiency bifunctional catalysts for electrosynthesis of ethanol into high value-added multicarbon compound coupled with hydrogen production. *J. Am. Chem. Soc.* 143 (29), 10822–10827.
- You, B., Han, G., Sun, Y., 2018. Electrocatalytic and photocatalytic hydrogen evolution integrated with organic oxidation. *Chem. Commun.* 54 (47), 5943–5955.
- You, B., Liu, X., Jiang, N., Sun, Y., 2016. A general strategy for decoupled hydrogen production from water splitting by integrating oxidative biomass valorization. *J. Am. Chem. Soc.* 138 (14), 13639–13646.
- You, B., Sun, Y., 2018. Innovative strategies for electrocatalytic water splitting. *Acc. Chem. Res.* 51 (7), 1571–1580.
- Zhang, H., Tian, W., Duan, X., Sun, H., Liu, S., Wang, S., 2019. Catalysis of a single transition metal site for water oxidation: From mononuclear molecules to single atoms. *Adv. Mater.* 32 (18), 1904037.
- Zhang, J., Wang, Y., Yang, C., Chen, S., Li, Z., Cheng, Y., Wang, H., Xiang, Y., Lu, S., Wang, S., 2021a. Elucidating the electro-catalytic oxidation of hydrazine over carbon nanotube-based transition metal single atom catalysts. *Nano Res.* doi:10.1007/s12274-021-3397-9.
- Zhang, Q., Kazim, F.M.D., Ma, S., Qu, K., Li, M., Wang, Y., Hu, H., Cai, W., Yang, Z., 2021b. Nitrogen dopants in nickel nanoparticles embedded carbon nanotubes promote overall urea oxidation. *Appl. Catal.* B. 280, 119436.
- Zhang, Y., Qiu, Y., Ma, Z., Wang, Y., Zhang, Y., Ying, Y., Jiang, Y., Zhu, Y., Liu, S., 2021c. Core-corona Co/Co<sub>3</sub> clusters strung on carbon nanotubes as a Schottky catalyst for glucose oxidation assisted H<sub>2</sub> production. *J. Mater. Chem. A* 9 (17), 10893–10908.
- Zhao, B., Liu, J., Xu, C., Feng, R., Sui, P., Luo, J.-X., Wang, L., Zhang, J., Luo, J.-L., Fu, X.-Z., 2021a. Interfacial engineering of Cu<sub>2</sub>Se/C<sub>60</sub>Se<sub>4</sub> multivalent hetero-nanocrystals for energy-efficient electrocatalytic co-generation of value-added chemicals and hydrogen. *Appl. Catal.* B. 285, 119800.
- Zhao, B., Liu, J., Xu, C., Feng, R., Sui, P., Wang, L., Zhang, J., Luo, J.-L., Fu, X.Z., 2020a. Hollow NiSe nanocrystals heterogenized with carbon nanotubes for efficient electrocatalytic methanol upgrading to boost hydrogen co-production. *Adv. Funct. Mater.* 31 (8), 2008812.

- Zhao, B., Sun, M., Chen, F., Shi, Y., Yu, Y., Li, X., Zhang, B., 2020b. Unveiling the activity origin of iron nitride as catalytic material for efficient hydrogenation of CO<sub>2</sub> to C<sub>2+</sub> hydrocarbons. *Angew. Chem. Int. Ed.* 60 (9), 4496–4500.
- Zhao, H., Lu, D., Wang, J., Tu, W., Wu, D., Koh, S.W., Gao, P., Xu, Z.J., Deng, S., Zhou, Y., You, B., Li, H., 2021b. Raw biomass electroreforming coupled to green hydrogen generation. *Nat. Commun.* 12 (1), 2008.
- Zhao, T., Wang, Y., Karuturi, S., Catchpole, K., Zhang, Q., Zhao, C., 2020c. Design and operando/in situ characterization of precious-metal-free electrocatalysts for alkaline water splitting. *Carbon Energy* 2 (4), 582–613.



**Zhijie Chen** received his B.S. and M.S. degrees from the Wuhan University of Technology in 2015 and 2018, respectively. He is currently pursuing his Ph.D. degree at the University of Technology Sydney. His research work focuses on the eco-design of nanomaterials for advanced energy/environmental applications.



**Prof. Bing-Jie Ni** received his Ph.D. degree in environmental engineering in June 2009. He joined the Technical University of Denmark as a postdoctoral research fellow in September of 2009 and then joined The University of Queensland in February 2011 as a senior research fellow. He currently is a full professor in environmental engineering. He has been working in the field of renewable energy production, particularly the interface between chemical engineering and environmental technology. His work focuses on the integration of these disciplines to develop innovative and sustainable technological solutions to achieve efficient energy generation from renewable resources.